PRAMANA
journal of
physics

© Printed in India

Supplement to Vol. 45
October 1995
pp. 117-140

# Determination of mass and width of $W$ at LEP200

S. N. GANGULI
Tata Institute of Fundamental Research, Bombay 400 005.

## 1. Introduction

Large Electron Positron collider (LEP) at CERN, Geneva, is in operation since September 1989. There are four mammoth detectors - ALEPH, DELPHI, L3 and OPAL- which are collecting data at LEP. The purpose of LEP is to study the $Z^0$ during LEP100 Phase ( 1989-1995 ) at $\sqrt{s} \simeq 90$GeV. By the end 1993 each of the four detectors collected a total number of $Z^0$ events $\simeq 2 \times 10^6$ . Some of the results from these studies are [1]:

(a) **Mass of $Z^0$** is measured to a precision of $\frac{\Delta m}{m} = 10^{-4}$.
(b) **Number of light $\nu$** is measured as $N_\nu = 3.00 \pm 0.03$.
(c) Effective value of the electroweak mixing angle is measured to be $\sin^2\theta_{\text{eff}} = 0.2321 \pm 0.0006$.
(d) **Running of $\alpha_s$** is established at LEP.
(e) **Top mass** is estimated to be $166^{+17}_{-19} \pm 20$ GeV
(f) **Lower limit** on Higgs boson mass is 63.5 GeV
(g) **Standard Model** of EW interactions is tested at LEP to a precision better than 0.5 %.

LEP200: The second phase of LEP, sometimes called LEP200 phase, is to achieve centre of mass energy for $e^+e^-$ collision above the W production threshold so as to observe and study for the first time the reaction

$$e^+e^- \rightarrow W^+W^- \tag{1}$$

It may be recalled that one of the main reasons for the need of $Z^0$ is to regularise the production cross section of $W^+W^-$; without the $Z^0$ the energy dependence of the cross section violates unitarity bound, fig 1.

Beam Energy: The upgradation of the LEP beam energy from $\simeq$ 45 GeV to above the W mass threshold will be achieved by adding 192 superconducting RF cavities in the LEP ring. This will lead to $E_{\text{beam}} = 88$ GeV yielding centre of mass energy for collision as $\sqrt{s} = 176$ GeV.

Luminosity: The expected luminosity is $4 \times 10^{31}\text{cm}^{-2}\text{sec}^{-1}$. With the running period of $\simeq$ 6 months a year for LEP, the integrated luminosity in a year will be $\simeq 240\text{pb}^{-1}$. Total approved luminosity at LEP200 is expected to be $500\ \text{pb}^{-1}$. With $\sigma\ (e^+e^- \rightarrow W^+W^-) \simeq 16$pb, the number of expected W pairs per experiment will be $\simeq 8000$.

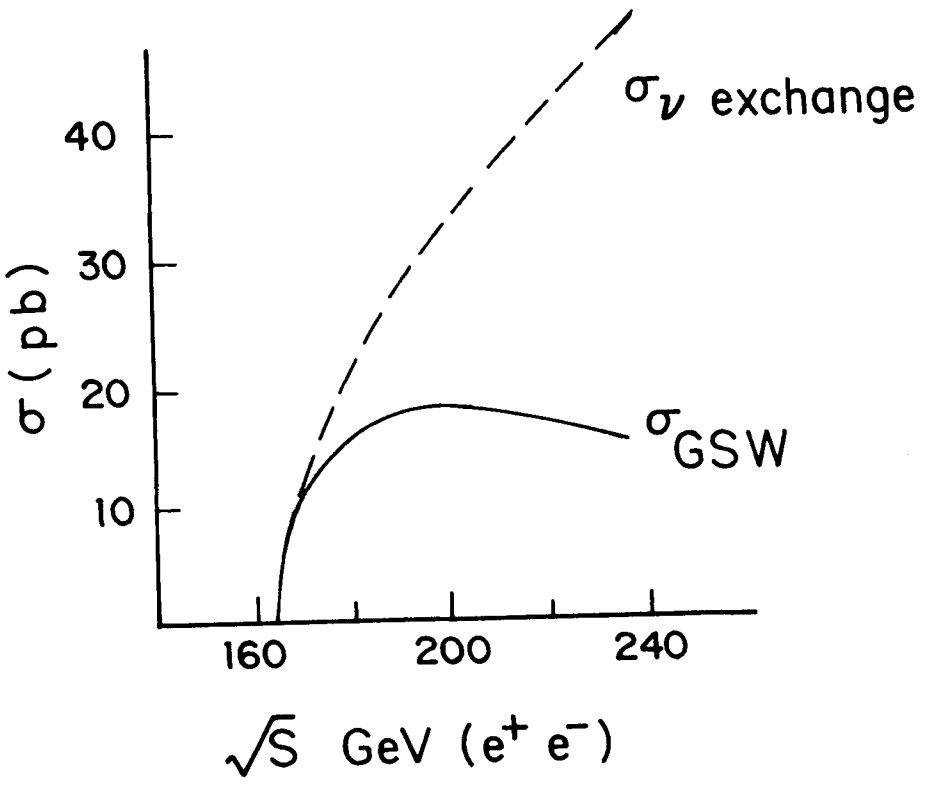


**Figure 1.** Production cross section of $e^+e^- \rightarrow W^+W^-$ as a function of $\sqrt{s}$. Dotted line is for only $\nu$ exchange while the solid line is from the Standard Model.

Aims of LEP200: The physics capabilities of LEP200 have been extensively studied [2, 3]. There are however three main topics: (a) Precision measurement of $M_W$ and $\Gamma_W$; (b) Determination of Triple Gauge Boson couplings, and (c) Search of New Particles. In this talk we will restrict ourselves to the first topic.

## 2. Prsent knowledge of $M_W$ and $\Gamma_W$

**Present knowledge of $M_W$**: Mass of W has been measured in two ways:

(i) Direct Measurements

Experiments at $\bar{p}p$ colliders, UA2 and CDF, made direct measurements [4] of the W mass from $W \rightarrow l\nu$ events. Their results are summarised below.

$$M_W/M_Z = 0.8813 \pm 0.0036 \pm 0.0019 \text{ GeV (UA2)}$$
$$M_W = 79.91 \pm 0.39 \text{ GeV (CDF)}$$

The combined result is: $\boxed{M_W = 80.22 \pm 0.26 \text{ GeV}}$

(ii) Indirect Estimation

The LEP data consisting of energy dependence of various cross sections ( $e^+e^- \rightarrow Z^0$ and $Z^0 \rightarrow$ hadrons, $e^+e^-$, $\mu^+\mu^-$ and $\tau^+\tau^-$) and asymmetries when fitted in the framework of the Standard Model leads to the mass of W and this value is [1]:

$$M_W = 80.25 \pm 0.10 \pm 0.03 \text{ GeV (LEP)}$$

[ Second error due to variation of Higgs between 60-1000 GeV]

**Present knowledge of $\Gamma_W$**: The W width as quoted by UA2, UA1 and CDF experiments [4] **are not direct measurements**; the width is **'extracted'** from the measurement of R

$$R = \sigma(W \rightarrow e\nu)/\sigma(Z \rightarrow e^+e^-) \quad (2)$$
$$(3)$$
$$= \frac{\sigma(\bar{p}p \rightarrow W + X)}{\sigma(\bar{p}p \rightarrow Z + X)} \cdot \frac{\Gamma(W \rightarrow e\nu)}{\Gamma(Z \rightarrow e^+e^-)} \cdot \frac{\Gamma_Z}{\Gamma_W} \quad (4)$$

The quantities $\sigma(\bar{p}p \rightarrow W + X)/\sigma(\bar{p}p \rightarrow Z + X)$ and $\Gamma(W \rightarrow e\nu)/\Gamma(Z \rightarrow e^+e^-)$ are calculated from theory, and $\Gamma_Z$ is taken from LEP measurements.

Values from the three collider experiments are summarised below:

$$\Gamma_W = 2.10 \pm 0.14 \pm 0.09 \text{ GeV (UA2)} \quad (5)$$
$$\Gamma_W = 2.18 \pm 0.26 \pm 0.04 \text{ GeV (UA1)} \quad (6)$$
$$\Gamma_W = 2.12 \pm 0.20 \text{ GeV (CDF)} \quad (7)$$

The combined result is: $\boxed{\Gamma_W = 2.12 \pm 0.11 \text{ GeV}}$

## 3. Why the precision mesaurement of $M_W$

W is a vector gauge boson and therefore the knowledge of its mass is very important. Some of the other reasons are:

[A] It may be recalled that the top quark and the Higgs boson are the two unknowns in the Standard Model. Precision measurement of $M_W$ will give further constraints on the mass of the Higgs if the top quark mass is known, fig. 2, [5].

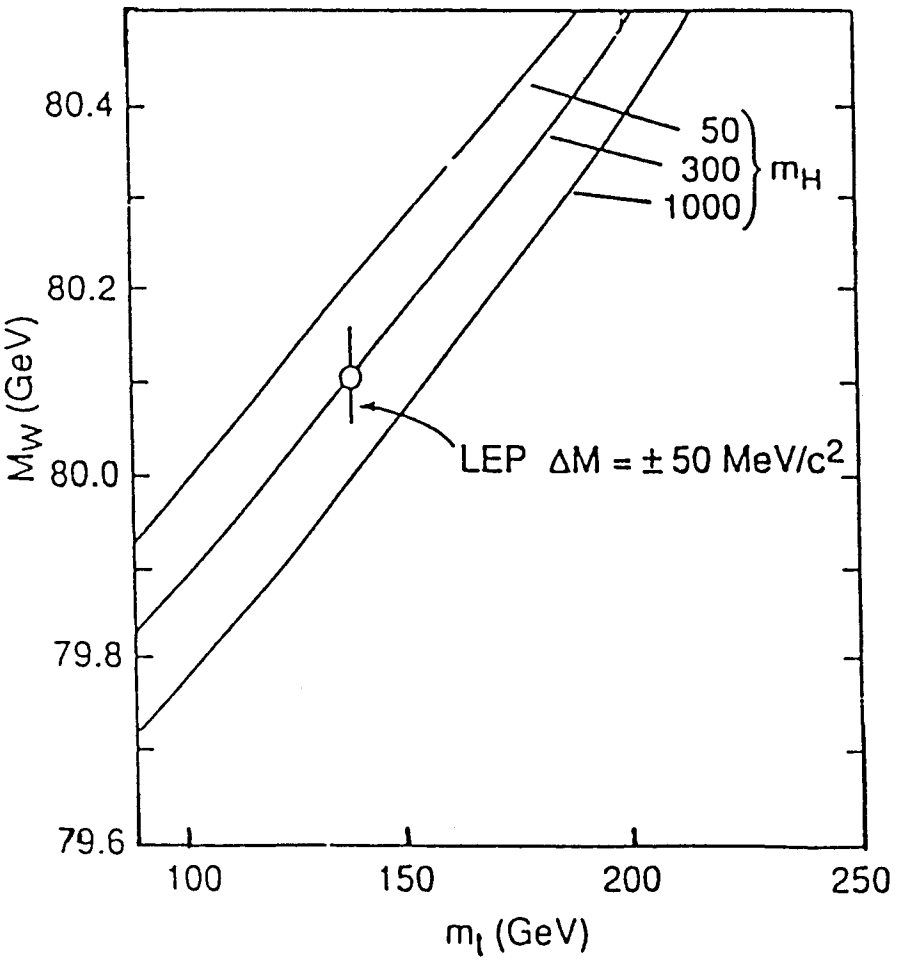


**Figure 2.** $M_W$ vs $M_{top}$ curves in the framework of the Standard Model for three different values of Higgs mass.

For example if Top mass is known from hadron collider experiments at Fermilab (a) with a precision of $\Delta M_{top} = 10$ GeV, then 50 MeV error on W mass measurement will lead to $\Delta M_{Higgs} = ^{+340}_{-170}$ GeV, and (b) precision in $\Delta M_{top} = 2$ GeV and 50 MeV in $M_W$ will yield $\Delta M_{Higgs} = ^{+176}_{-118}$ GeV.

### [B] Testing radiative corrections

Radiative corrections come from self energies , formfactors, box diagrams etc. The mass of the W and Z are related by,

$$M_W^2 = \frac{\pi\alpha}{\sqrt{2}G_F(1 - M_W^2/M_Z^2)} \cdot \frac{1}{1 - \Delta r} \tag{8}$$

The error in the radiative correction $\Delta r$ arises mainly from the error in $M_W$ as the value of $M_Z$ is known to a very high precision ($\Delta M_Z = 6$ MeV). The error of 50 MeV in $M_W$ will lead to error on $\Delta r$ as 0.003.

It may be noted that the radiative correction $\Delta r$ depends on $M_{top}$ and$M_{Higgs}$ and hence can be determined independent of $M_W$. The L3 experiment [6] at LEP has determined the value of $\Delta r = 0.045 \pm 0.013$.

Two ways of determining radiative corrections as mentioned above can thus be compared.

## 4. *W* production mechanism

Leading order diagrams are due to Z, $\gamma$ and $\nu$ exchanges and their interferences.

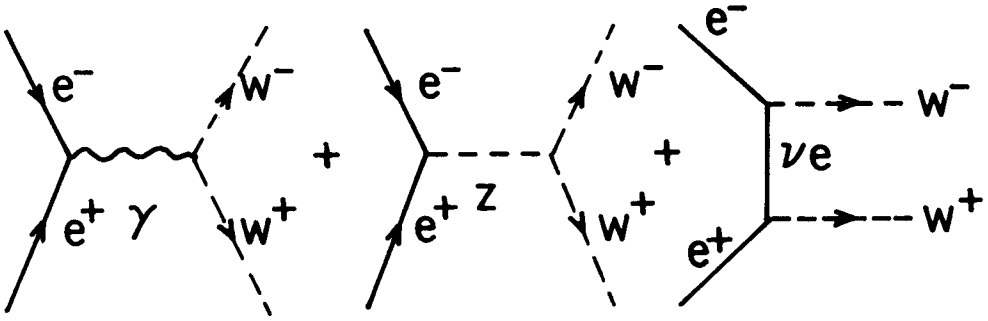


Initial state helicities are LR or RL for the Z and $\gamma$ exchanges, while only the LR diagram is allowed for the $\nu$ exchange (since $\nu$ is left handed). It may be noted that the $\nu$ diagram is the dominant one and as a result $W^+$ and $W^-$ are peaked along the $\vec{p}_{e+}$ and $\vec{p}_{e-}$ directions respectively, fig.3.

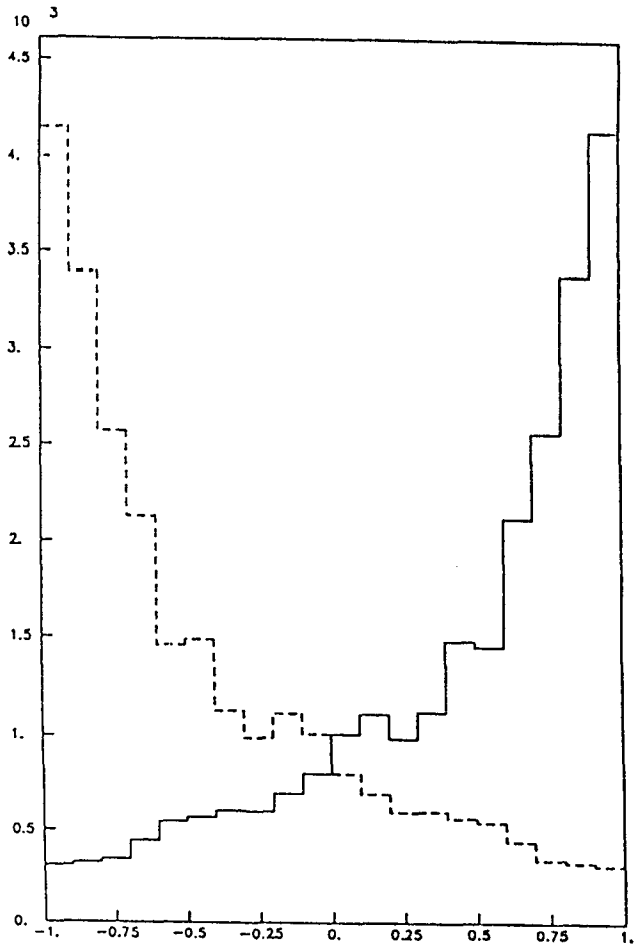


$\cos\theta_{(e^+W)}$ distributions for $W^+$ (continuous line) and $W^-$ (dashed line).

**Figure 3.** Angular distribution of $W^+$ and $W^-$ with respect to the direction of $e^+$ beam.

For the forward-backward production the longitudinal component of the W helicity ($\lambda = 0$) is equally important as the transverse states ($\lambda = +1$ *or* $-1$).

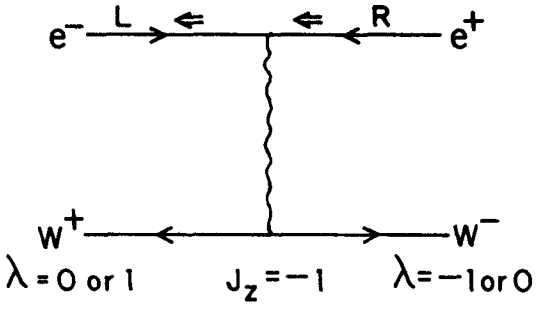


## 5. *W* decay modes

Final states from $e^+e^- \rightarrow W^+W^-$ are classified into three classes depending on W decay modes

| | | |
|---|---|---|
| Pure Leptonic : | $WW \rightarrow l\nu l\nu$ : | 7.5 % |
| Semi Leptonic : | $WW \rightarrow l\nu q\bar{q}$ : | 40 % |
| Pure Quark : | $WW \rightarrow q\bar{q}q\bar{q}$ : | 52.5 % |

A quark from W decay will undergo fragmentation/hadronization leading to a formation of jet in the final state.

### Topology of WW events

(i) Since the $W^+$ and $W^-$ are peaked along $\vec{p}_{e^+}$ and $\vec{p}_{e^-}$ respectively and hence the charged leptons from W decay will reflect the parents angular distributions.

(ii) Pure Leptonic Mode: Two visible leptons or a thin jet from the hadronic decay of $\tau$ will be seen in the final state.

(iii) Semi-leptonic decay : Two jets and one isolated lepton or, two jets and one thin jet in the final state.

(iv) Pure Quark decay : Four jets or more in the final state.

## 6. Main sources of background

Production cross-section of $W^+W^-$ process is $\simeq$ 16pb. In this section we discuss briefly several sources of some of the background and they are:

(i) $e^+e^- \rightarrow Z\,Z \rightarrow f\bar{f}$ :

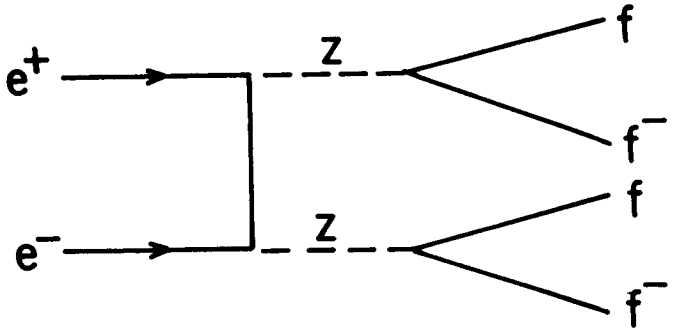


Total yield of this reaction is only a few % of the WW signal.

(ii) $e^+e^- \rightarrow f\,\bar{f}$:

The cross-section is 10 pb for f = lepton and leads to nearly back to back leptons which can be removed by an appropriate cut. The cross-section is 26 pb for f = quark, but then this reaction is dominated by 2 and 3 jets, while WW signal leads to 4 or more jets.

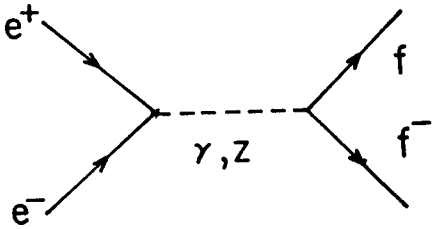


(iii) $e^+e^- \rightarrow f\,f\,\gamma$

This reaction is due to on-mass shell $Z^0$ exchange with monochromatic $\gamma$ of $\simeq$ 70 GeV. Cross section for this reaction is 80 pb for f = quark & 20 pb for f = lepton; Major fraction of these events can be rejected from large missing momentum.

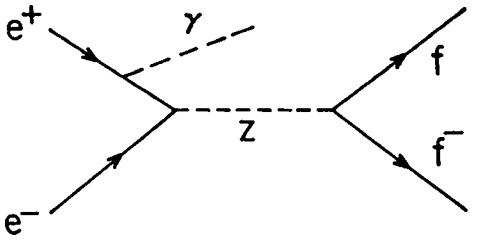

(iv) $e^+e^- \rightarrow e^+e^-e^+e^-$ $(\mu^+\mu^-)$

This reaction will have two leading electrons which are lost in the beam pipe. Missing $p_T$ and acoplanarity will remove most of this background.

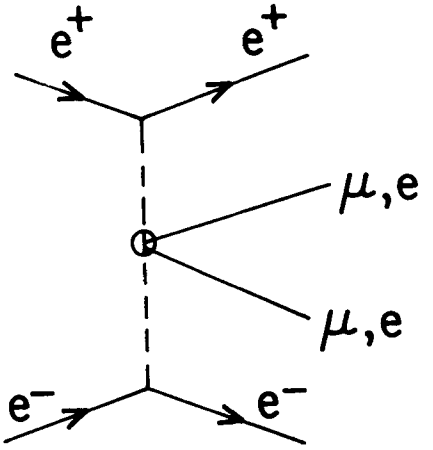


## 7. Experimental methods to measure $M_W$

Three methods have been discussed in the literature and they are:

[A] Direct Reconstruction:

W's are reconstructed using either hadronic events, where both W decay into jets, or hadronic-leptonic events, where one W decays hadronically while the other into leptonic mode.

**Note that the masses of the two W's produced will have different masses due to finite width of W.** Some of the groups have assumed equal masses for reconstructing W's [5]. In L3 we have assumed unequal masses for reconstructing W's.

[B] **Shape of the Excitation Curve**:

From the measured shape of the production cross section one deduces the value of $M_W$.

[C] **Lepton end point energy**:

The value of $M_W$ is obtained from the lepton spectrum of leptonic decays of W's

## 8. W pair generators

To carry out simulation studies we need Monte Carlo programs that generate $e^+e^- \rightarrow W^+W^-$ events. There are several generators available and they are summarised in Table 1. Some of the important ingredients used in a generator like inclusion of W width, proper implementation of CKM matrix elements, incorporation of the initial state radiation, flexibility in triple gauge boson coupling, and hadronization scheme are also indicated in Table 1.

**Table 1.**

| Generator | Herwig | Pythia | LEPWW | GENTLE | WWgamma |
|---|---|---|---|---|---|
| $\Gamma_W$ | Y | Y | Y | Y | Y |
| $V_{CKM}$ | Y | Y | N | Y | Y |
| ISR | N | Y | Y | Y | hard photon |
| General ZWW, $\gamma$WW | N | N | Y | N | N |
| Hadronization | Cluster | LUND | LUND | LUND | LUND |
| Author | Webber | Sjostrand | Kleiss | Bardin | KEK-LAPP |

REMARKS: GENTLE [7] makes a detailed implementation of ISR taking into account t-channel exchange diagrams properly.

## 9. Jet reconstruction algorithms

When both the Ws decay by hadronic mode, one recombines the hadrons to make four jets; each jet representing a parent quark. Since the W's are slow ($\beta \simeq 0.5$), the hadrons of a given jet are not well separated from those of other jets. Therefore a reconstructed jet may have particles of another jet. When one W decays hadronically and the other via leptonic mode then the number of jets is reduced and the mismatch is much less.

There are several different algorithms for the reconstruction of jets. Below we discuss six different algorithms.

(i) Generator History:

In this procedure one recombines the hadrons, belonging to a given quark, to form a jet. Therefore no mismatch of particles between different jets. This is possible because we are dealing with generated events.

(ii) Jade algorithm [8] :

$$y_{ij} = \frac{2E_iE_j(1-\cos\theta_{ij})}{E_{vis}^2} \tag{9}$$

The quantity $y_{ij}$ is based on invariant mass squared of 'jets' i and j (to start with one uses small resolvable cluster as a jet). $E_i$ and $E_j$ are energies of jets with $\theta_{ij}$ and $E_{vis}$ as opening angle and total visible energy respectively. The pair of jets with the smallest $y_{ij}$ are combined into a new jet and all $y'_{ij}$s are recalculated; this procedure is repeated iteratively until we are left with four jets. The exact definition of $y_{ij}$ is different in (iii), (iv) and (v) below.

(iii) Durham algorithm [9]:

$$y_{ij} = \frac{2Min(E_i^2, E_j^2)(1-\cos\theta_{ij})}{E_{vis}^2} \tag{10}$$

(iv) Geneva algorithm [10]:

$$y_{ij} = \frac{8E_iE_j(1-\cos\theta_{ij})}{9(E_i+E_j)^2} \tag{11}$$

(v) Lund algorithm [11]:

$$y_{ij} = \frac{2|\vec{p_i}||\vec{p_j}|\sin\frac{\theta}{2}}{|\vec{p_i}+\vec{p_j}|} \tag{12}$$

(vi) Generalised thrust approach [12] : Thia approach has been used at PETRA to study 4 jet events. The aim is to find four jet axes as the unit vectors $\hat{n}_j$ so that a generalised form of the standard thrust

$$T_4 = Max\left(\frac{\sum_i \max_i(\vec{p_i}\cdot\hat{n}_j)}{\sum_i|\vec{p_i}|}\right) \tag{13}$$

is maximised.

## 10. $M_W$ from direct measurement

There are three types of events:
(i) **Pure Quark or** 'HadronicDecay : $W^+ W^- \rightarrow q_1\,\bar{q}_2\,q_3\,\bar{q}_4$

(ii) **Semi Leptonic Decay** : (a) $W^+ W^- \rightarrow q_1\,\bar{q}_2\,e\,\nu_e$ , (b) $W^+ W^- \rightarrow q_1\,\bar{q}_2\,\mu\,\nu_\mu$
(c) $W^+ W^- \rightarrow q_1\,\bar{q}_2\,\tau\,\nu_\tau$

(iii) **Pure Leptonic Decay** : $W^+ W^- \rightarrow l\,\nu_l\,l'\,\nu_{l'}$

Energy and momentum conservation of the reaction can be made if we are able to measure 4-momentum vectors of all the final products. This will result in fits with 4 constraints. Experimentally one will be able to measure (a) 4-momentum

vectors of the jets formed from quarks, (b) 4-momentum vectors of e and $\mu$ and (c) direction of $\tau$ from its decay products. Quantities that we cannot measure are (a) $\nu$ momentum as it is not detected; this decreases the number of constraint by three, and (b) energy of $\tau$ as its decay involves $\nu$ corresponding to a decrease of one constraint.

Keeping in mind the above points we will not presently use (iic) and (iii) for our kinematic fits.

## 10.1 Details of Kinematic Fitting :

As mentioned earlier one carries out kinematic fits to impose energy momentum conservation. Constraint equations are described in detail below.

(i) $WW \rightarrow (j_1j_2)(j_3j_4)$

Constraint equations are $\Longrightarrow$

$$\begin{aligned}
&(1)\ E_{j1} + E_{j2} + E_{j3} + E_{j4} - \sqrt{s} = 0 \\
&(2)\ p^x_{j1} + p^x_{j2} + p^x_{j3} + p^x_{j4} = 0 \\
&(3)\ p^y_{j1} + p^y_{j2} + p^y_{j3} + p^y_{j4} = 0 \\
&(4)\ p^z_{j1} + p^z_{j2} + p^z_{j3} + p^z_{j4} = 0
\end{aligned}$$

Besides the above 4 constraints, two more constraints can be used if one assumes equal masses for the two W's

$$\begin{aligned}
&(5)\ (E_{j1} + E_{j2})^2 - (\vec{p}_{j1} + \vec{p}_{j2})^2 - M_W^2 = 0 \\
&(6)\ (E_{j3} + E_{j4})^2 - (\vec{p}_{j3} + \vec{p}_{j4})^2 - M_W^2 = 0
\end{aligned}$$

With unknown as $M_W$ one ends up with 5C fit.

(ii) $WW \rightarrow (j_1j_2)(l\nu)$

Repeating the procedure as described in (i) yields 2C fit for this reaction.

**Remark**: Allowing the two W masses to be unequal one ends up with 4C and 1C fits respectively

## 10.2 Effect of initial state radiation

Initial state radiation (ISR) is a common feature in $e^+e^-$ interactions i.e., the $e^-$ emits a photon in the presence of the Coulomb field of the $e^+$ or vice versa. The distribution in the photon energy from ISR is shown in fig.4 from the GENTLE generator and its mean value is: $< E_{rad} >= 1.211$GeV at $\sqrt{s} = 176$ GeV.

The effect of ISR in the cross section for $e^+e^- \rightarrow W^+W^-$ is incorporated as follows:

**Without ISR** the cross-section is given by [13]:

$$\sigma(s) = \int_0^s dm_1^2 \cdot \rho(m_1) \int_0^{(\sqrt{s}-m_1)^2} dm_2^2 \cdot \rho(m_2) \cdot \sigma_0(s; m_1, m_2) \qquad (14)$$

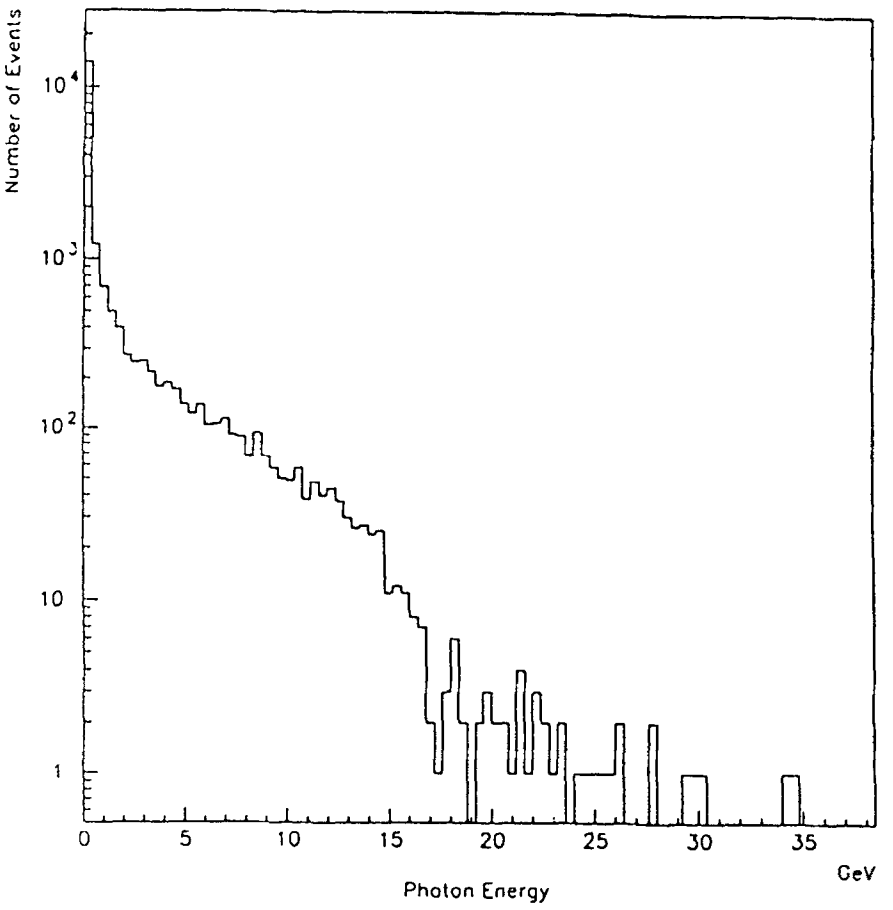


**Figure 4.** Energy distribution of ISR photons.

$$\rho(m) = \frac{1}{\pi M_W} \cdot \frac{m^2 \Gamma_W}{(m^2 - M_W^2)^2 + m^2 \Gamma_W^2} \tag{15}$$

$M_W$ and $\Gamma_W$ are the mass and width of W; $m_1$ and $m_2$ are the two produced W masses and $\rho(m)$ is the Breit-Wigner (BW) distribution. $\sigma_0(s; m_1, m_2)$ is the Born cross section [13] at the centre of mass energy of $\sqrt{s}$.

**With ISR** the cross-section is given by [7]:

$$\sigma(s) = \int_0^s dm_1^2 \cdot \rho(m_1) \int_0^{(\sqrt{s}-m_1)^2} dm_2^2 \cdot \rho(m_2) \cdot \overline{\sigma}(s, s') \tag{16}$$

$$\overline{\sigma}(s, s') = \int_0^{1-(m_1+m_2)^2/s} dx \cdot \sigma_0(s(1-x)) \cdot H(x, s) \tag{17}$$

$$H(x, s) = \beta \cdot x^{(\beta-1)} \cdot (1 + \overline{S}) + \overline{H} \tag{18}$$

$$\overline{S} = \frac{\alpha}{\pi}[\frac{\pi^2}{3} - \frac{1}{2}] + \frac{3}{4}\beta + \mathcal{O}(\alpha^2) \tag{19}$$

$$\overline{H} = -\beta(1 - x/2) + \mathcal{O}(\alpha^2) \tag{20}$$

$$\beta = \frac{2\,\alpha}{\pi}[\log(s/m_e^2) - 1] \tag{21}$$

H(x,s) is the radiator function [14] and x is a fractional momentum carried by the photon.

From the two distributions, eqs.(14) and (16), we calculated the average value of mass, $< (m_1 + m_2)/2 >$ and the mass difference $|m_1 - m_2|$ and they are listed below.

| Parameters | $Q_0$ Without ISR (GeV) | $Q_1$ With ISR (GeV) | $Q_0$ - $Q_1$ (MeV) |
|---|---|---|---|
| Mass | 80.046 (3.19) | 79.972 (3.20) | 74.0 |
| $< (m_1 + m_2)/2 >$ | 79.835 (2.85) | 79.732 (2.93) | 103.0 |
| $\|m_1 - m_2\|$ | 3.292 (4.61) | 3.341 (4.77) | -49.0 |

**The effect of ISR [15]**: Finally we may conclude the following effect due to ISR on our distributions:

(a) To lower the mean values of mass and $< (m_1 + m_2)/2 >$ by 74 and 103 MeV respectively,

(b) To increase the dispersion by nearly 0.2%,

(c) To decrease the total cross section by $\simeq$ 2 pb.

## 10.3 Results from DELPHI study [5]

They have generated $\approx$ 3500 events of $W^+W^- \rightarrow$ 4jet and $\approx$ 1300 events of (2jet + $l\nu$) corresponding to $\approx 400 pb^{-1}$. Events were simulated through DELPHI detector. Jet reconstructions were carried out using generalised thrust algorithm.

Kinematic fit was carried out with the constraint that the two W masses are equal [5C & 2C fit for 4-jet & 2-jet+$e\nu_e$ respectively]. To extract $M_W$ from the data : fit was made with a BW of fixed width folded with a Gaussian (detector resolution function) plus a constant background.

**RESULTS**: Fitted mass distributions of W are shown in figs.5(a)-5(c) for three types of events: 4 jets, 2 jets + $\mu\nu$ and 2 jets + $e\nu$. They find a systematic positive offset of the fitted value of the mass with respect to true W mass used in the generator. This is summarised below:

$$\boxed{(\text{Fitted } M_W - M_W^{true}) = 422 \pm 79 \text{ MeV}, \quad (4\text{-jet})}$$
$$(\text{Fitted } M_W - M_W^{true}) = 819 \pm 160 \text{ MeV}, \quad (2 \text{ jet} + e)$$
$$(\text{Fitted } M_W - M_W^{true}) = 432 \pm 116 \text{ MeV}, \quad (2 \text{ jet} + \mu)$$

## Results from L3 study [15]

L3 collaboration has also carried out similar study but **without the detector simulation**. They have used events generated by GENTLE and quarks were allowed to undergo hadronization. Jets were then reconstructed **ignoring ISR photons**. Kinematic fits were carried out by ignoring the ISR photons.

Figs.6(a) and (b) show the distributions of (Fitted - Generated) mass for two cases: (i) for all events and (ii) for events with ISR photon energy $E_\gamma < 20$ MeV.
Mean values of the two distributions are:

$$\boxed{(\text{Fitted } M_W - M_W^{true}) = 477 \pm 16 \text{ MeV}, \quad (\text{all events})}$$
$$(\text{Fitted } M_W - M_W^{true}) = -11 \pm 7 \text{ MeV}, \quad (\text{events with } E_\gamma < 20 \text{ MeV.})$$

From the above results it is clear that (i) when there is no ISR photons (which is same as selecting events with $E_\gamma < 20$MeV) the value of (Fitted $M_W - M_W^{true}$) is consistent with zero, and (ii) when all events are used (and not using ISR photons in kinematic fits) one sees the positive offset as seen by DELPHI.

## Understanding the positive offset in $M_W$

The emmision of ISR actually reduces the effective centre of mass energy to $\sqrt{s'}$, which is lower than the nominal energy $\sqrt{s} = 2 \times E_{beam}$. If x is the fractional beam energy carried by the initial state photon then $\sqrt{s'} = s(1 - x)$.

But kinematic fits as discussed earlier assume nominal cm energy $\sqrt{s}$. This results in higher Fitted Mass and the positive offset can be written down as: $\Delta m = + <$

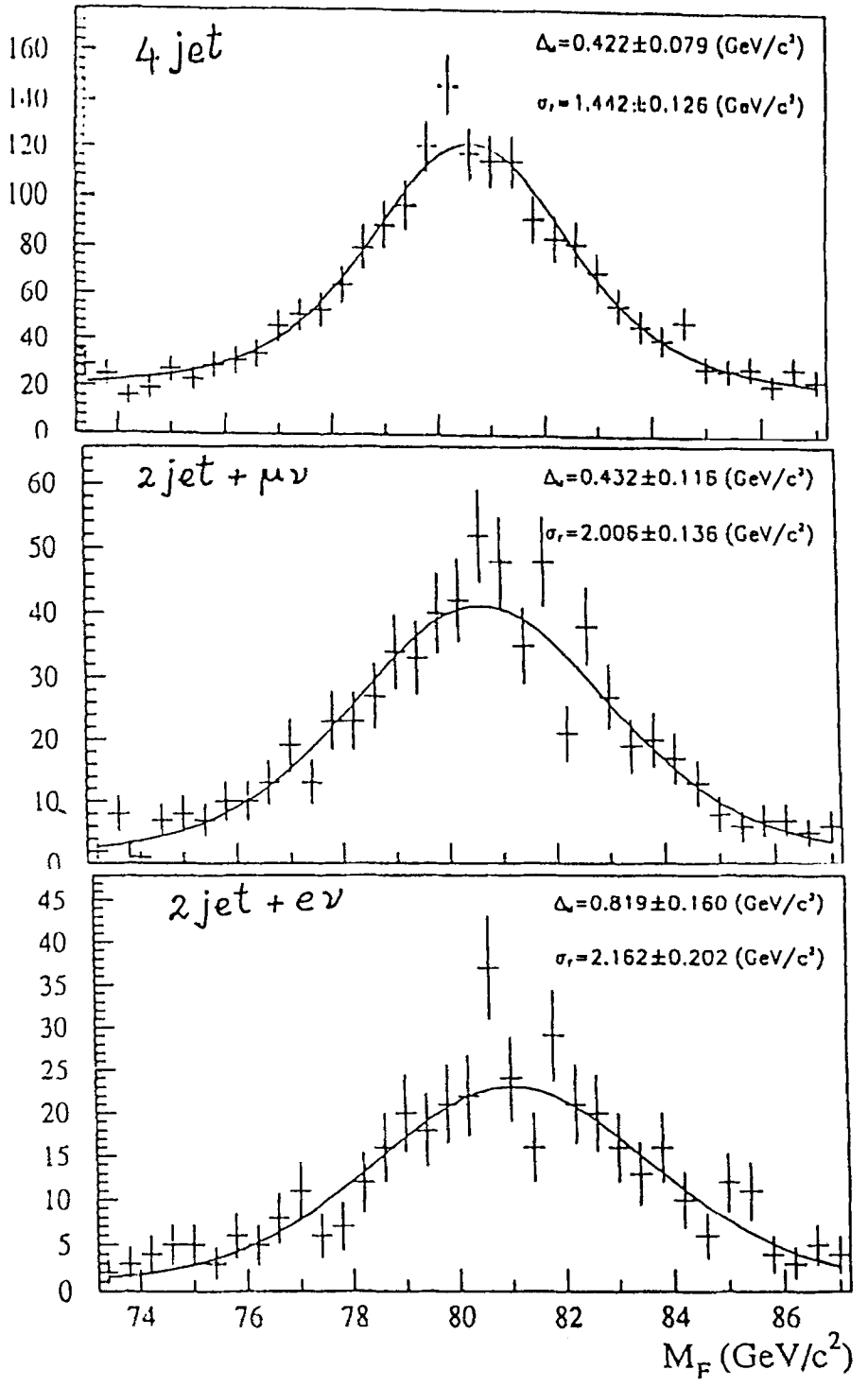


**Figure 5.** Fitted mass distributions of W for three types of events (a) 4 jets, (b) 2 jets + $\mu\nu$ and (c) 2 jets + e$\nu$.

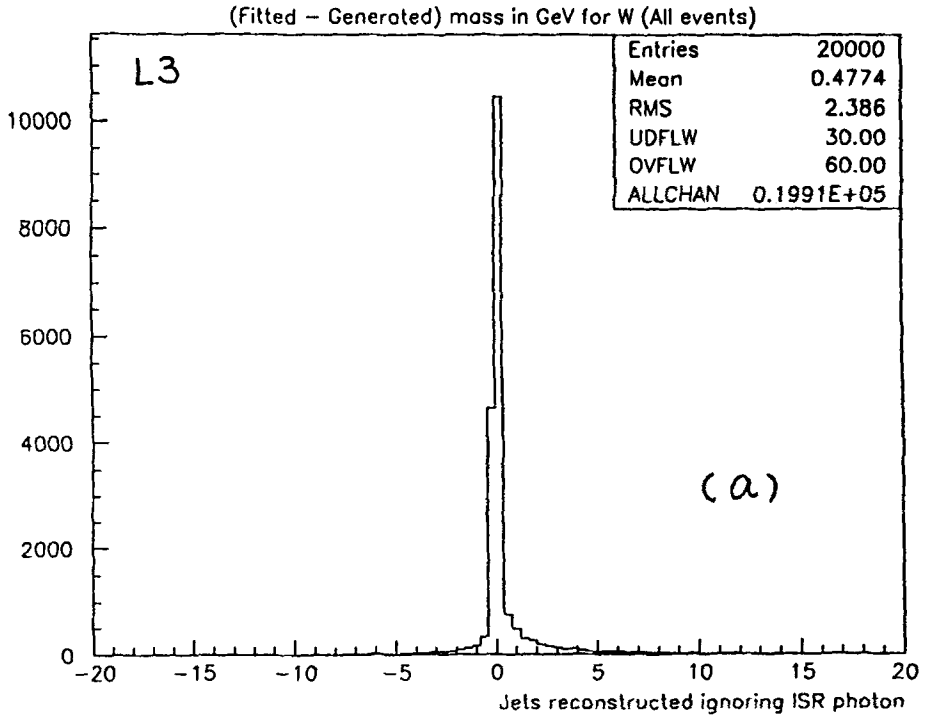


**Figure 6a.** (Fitted - generated) mass distribution for all events

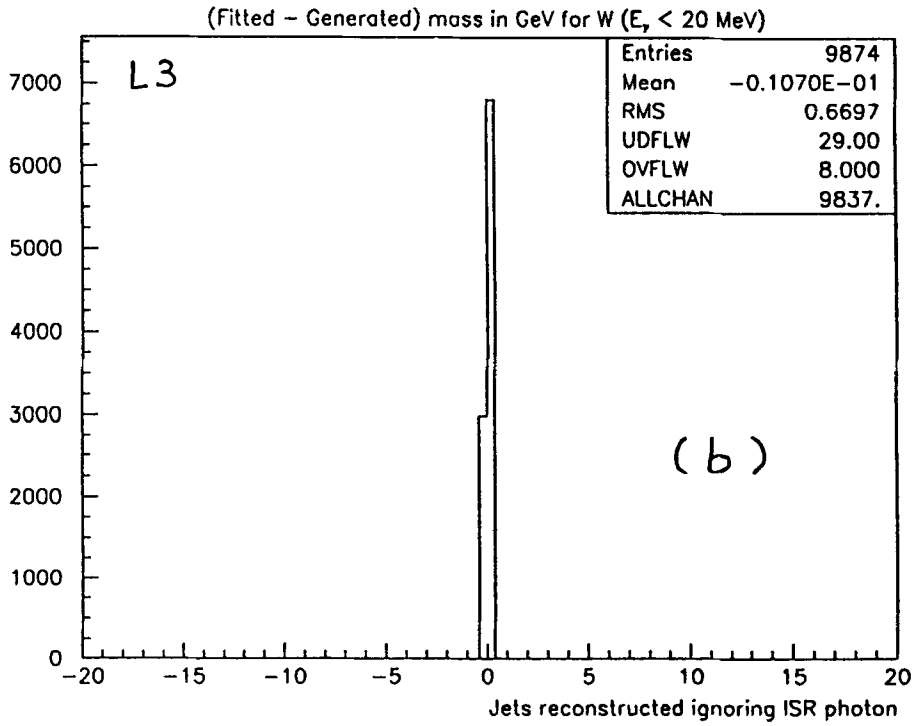


**Figure 6b.** (Fitted - generated) mass distribution for events with ISR photon energy $E_\gamma < 20$ MeV.

$E_{rad} > .\frac{M_W}{\sqrt{s}}$.

For $\sqrt{s} = 176$ GeV and the value of $< E_{rad} >= 1.2$ GeV yield $\Delta m = 500$ MeV.

**Shift in $M_W$ due to Reconstruction algorithm**

DELPHI collaboration repeated their fit analysis without ISR in the Monte Carlo and obtained (Fitted $M_W - M_W^{true}$) = $-130$ MeV. This is due to reconstruction algorithm and this needs to be done by other groups.

**Expected precision in $M_W$**

Projecting the Fit Analysis to $500pb^{-1}$ DELPHI estimated the expected precision in $M_W$ to be 55 MeV. Similar value for the precision has also been estimated by L3 [16], ALEPH & OPAL.

## 11. Simultaneous determination of $M_W$ and $\Gamma_W$ (L3) [17]

The analysis mentioned above was based on fitting equal mass to both the W, which is not technically right and also there is no straight way to determine the $\Gamma_W$.

L3 collaboration has proposed a strategy to determine simultaneously the mass and width of the W. They have used proper expression for the cross section involving convolution of two Breit-Wigner distributions weighted by tree level cross-section:

$$\sigma(s) = \int_0^s dm_1^2 \cdot \rho(m_1) \int_0^{(\sqrt{s}-m_1)^2} dm_2^2 \cdot \rho(m_2) \cdot \sigma_0(s; m_1, m_2) \tag{22}$$

$$\rho(m) = \frac{1}{\pi M_W} \cdot \frac{m^2 \Gamma_W}{(m^2 - M_W^2)^2 + m^2 \Gamma_W^2} \tag{23}$$

Distributions of mass, mass difference and mean mass are then given by

$$d\sigma/dm_1 = 4m_1\rho(m_1) \cdot \int_0^{(\sqrt{s}-m_1)} dm_2[m_2\rho(m_2)\sigma_0(s; m_1, m_2)] \tag{24}$$

$$d\sigma/d\Delta m = 8 \cdot \int_{0.5\Delta m}^{0.5\sqrt{s}} d < m > [m_1 m_2 \rho(m_1)\rho(m_2)\overline{\sigma}(s, s') \tag{25}$$

$$d\sigma/d < m > = 8 \cdot \int_0^{2<m>} d\Delta m[m_1 m_2 \rho(m_1)\rho(m_2)\overline{\sigma}(s, s') \tag{26}$$

Where $\Delta m = |m_1 - m_2|$, and $< m >= (m_1 + m_2)/2$

It is proposed to use either the variables $m_1$ and $m_2$ or $\Delta m$ and $< m >$. ISR has been incorporated in these expressions, see sect. 10.2.

**RESULTS**: Results are presented here at the generator level i.e., without simulating through the detector. Total event sample used was 10,000 events without

ISR from the generator GENTLE. Mass and width used in the generator were: $M_W = 80.220$GeV, and $\Gamma_W = 2.033$GeV.

We have carried out simultaneous fits to: (i) double mass distribution in $m_1$ & $m_2$ using maximum likelihood method [15], and (ii) $\Delta m$ & $< m >$ using $\chi^2$ minimisation method. Fits from (ii) are shown in fig.7. Values of our fits are shown in the Table 2.

**Table 2.**

| Fitted quantities | $M_W$ (GeV) | $\Gamma_W$ (GeV) |
|---|---|---|
| $\Delta m, < m >$ | $80.231 \pm 0.014$ | $2.038 \pm 0.022$ |
| $m_1, m_2$ | $80.194 \pm 0.012$ | $2.041 \pm 0.027$ |

At the generator level the errors on mass and width from 10,000 events are 14 and 27 MeV respectively. Estimated errors on mass and width with detector resolution are $\simeq 50$ MeV and $\simeq 100$ MeV respectively.

## 12. $M_W$ from the excitation curve

This approach utilises the energy dependence of the production cross section of $(W^+W^-)$. But it is difficult to disentangle the effect due to $M_{top}$, $M_{Higgs}$, possible new physics etc. on the cross section. Sensitivity of cross section on $M_W$ is shown [5] in the fig.8. Fractional change in cross section for change in mass by 100 and 200 Mev are shown. It is seen that the fractional change is less than 1% even for change in mass by 200 MeV for $\sqrt{s} > 172$ GeV. This method as it stands at present does not seem to be very useful.

## 13. $M_W$ from the lepton end-point energy

The lepton energy, $E_l$, from the decay of W is limited by $M_W$

$$E_l < E_+ = \tfrac{1}{2}E_b + \tfrac{1}{2}\sqrt{E_b^2 - M_W^2}$$

Here $E_b$ is the beam energy. The error on $M_W$ due to error $\Delta E_+$ on the end point is given by,

$$\Delta M_W = \frac{\sqrt{E_b^2 - M_W^2}}{M_W} \Delta E_+$$

Several studies, see e.g. [5], have been made from the distribution of the generated

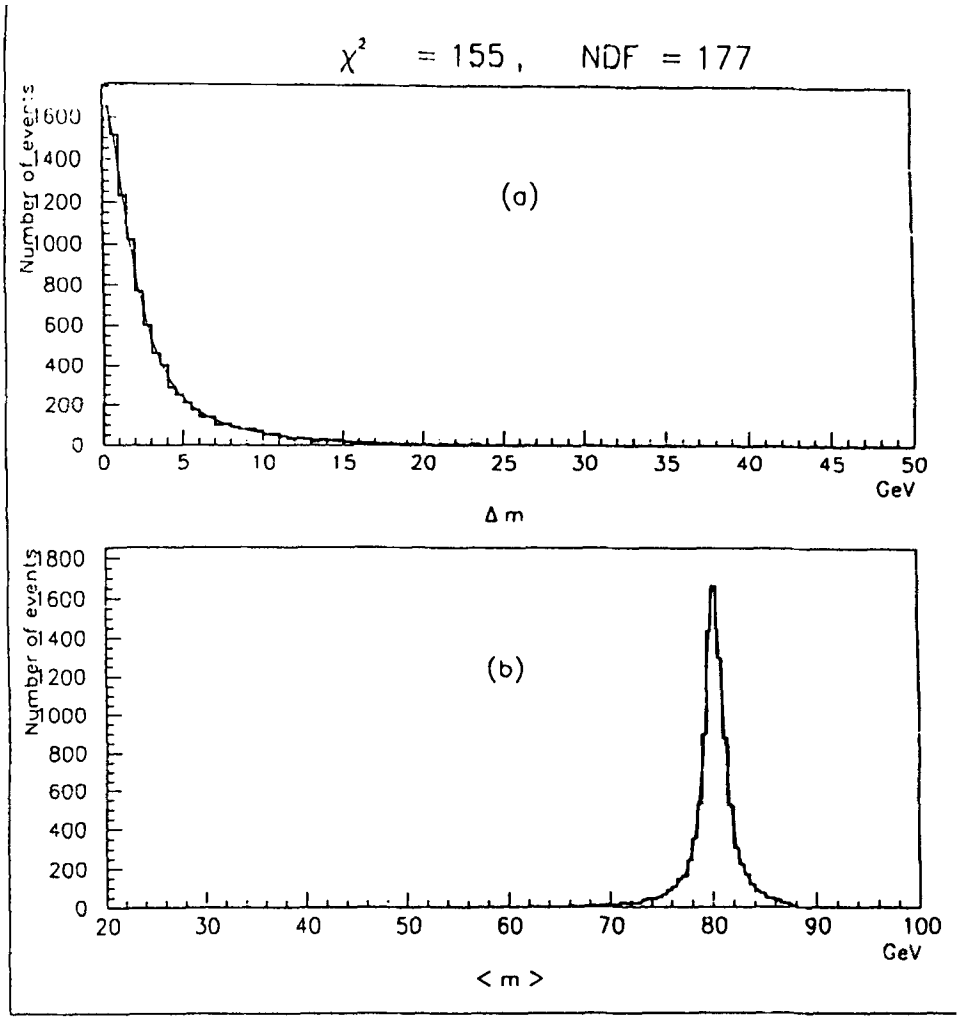


**Figure 7.** $\Delta m$ and $< m >$ distributions. Solid lines are simultaneous fits to the two distributions.

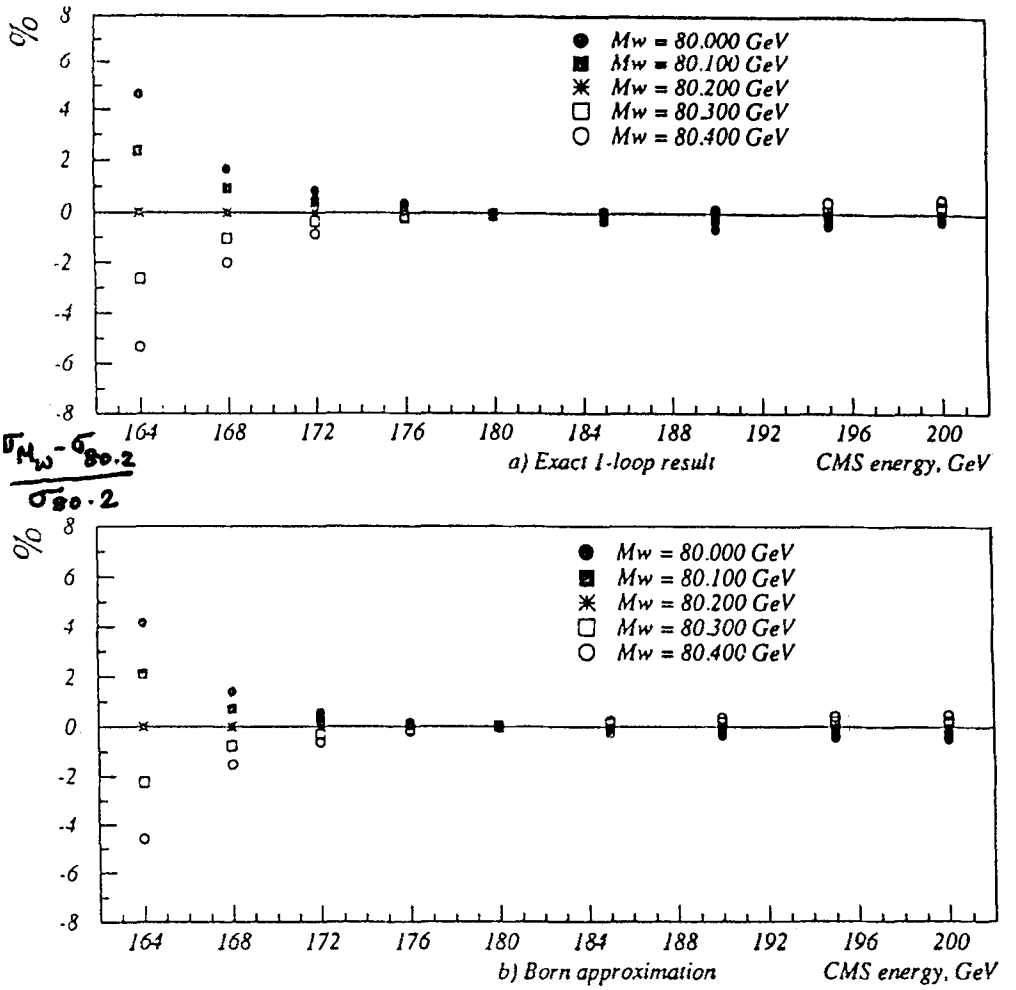


**Figure 8.** Fractional change in cross section as a function of $\sqrt{s}$. (a) Exact one loop result, and (b) Born approximation.

lepton energy and it is estimsted, see fig.9, that the error on $M_W$ from this method is expected to be,

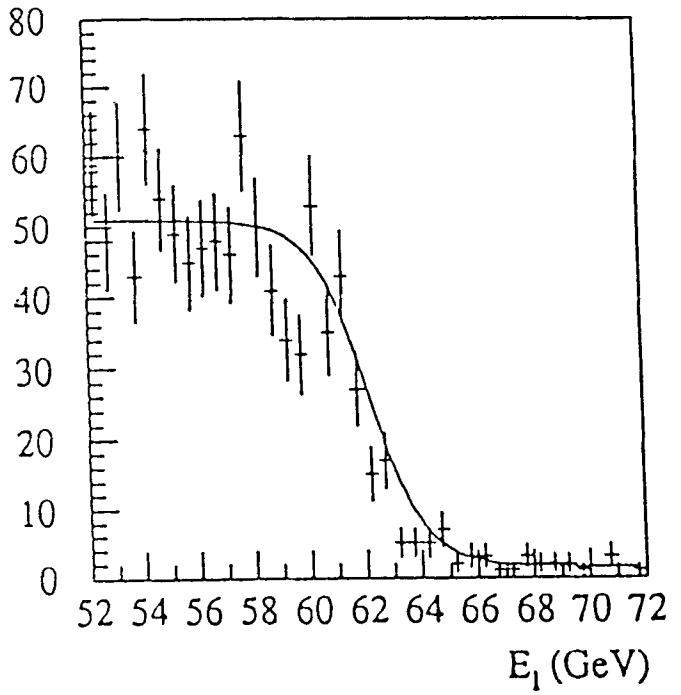


**Figure 9.** Lepton energy distribution from W→ $l\nu$.

$$\Delta M_W \approx 270\text{MeV}\sqrt{\frac{500\text{pb}^{-1}}{\epsilon\mathcal{L}}}$$

i.e., the error expected is more than 200 MeV.

## 14. Summary

- After a very useful run of physics at the $Z^0$ peak the reaction $e^+e^- \rightarrow W^+W^-$ will be studied at LEP200 starting from 1996.
- Longitudinal polarization of W will become available besides the transverse one.
- The approved integrated luminosity is 500 $pb^{-1}$ corresponding to $\simeq$ 8000 events.
- **Aims of LEP200**
  - (a) Precision measurement of $M_W$ and $\Gamma_W$
  - (b) Determination of Triple Gauge Boson couplings
  - (c) Search of New Particles
- Three methods have been studied regarding the measurement of $M_W$ and $\Gamma_W$ :

**[A] Direct Reconstruction**
**[B] Shape of the Excitation Curve**
**[C] Lepton end point energy**

Last two methods are not very useful.

- Precision expected for $M_W$ is $\simeq$ 50 MeV.
- Precision expected for $\Gamma_W$ is $\simeq$ 100 MeV.

## References


[1] The LEP Collaborations: 'Updated parameters of the $Z^0$ resonance from combined preliminary data of the LEP experiments: CERN/PPE/93-157, 26 August 1993.

[2] Proceedings of the ECFA Workshop on LEP200, CERN 87-08: D.H.Perkins, page 1; P.Roudeau et al., page 49; M.Davier et al., page 120.

[3] D.Treille, The LEP200 Programme: CERN-PPE 93-54, 26 March 1993.
L.Camilleri et al.: presentation at 1992 LEP200 Workshop, 2-4 November, 1992.

[4] Alitti et al.: CERN-PPE/91-208; CERN-PPE/91-162.
Abe et al.: Phys.Rev. D44(1991)29; Phys.Rev.Lett. 64(1990)152.
Albajar et al.: Phys.Lett. B253(1991)503.

[5] DELPHI Collaboration, D.Bardin et al.: DELPHI 92-166 PHYS 250(1992).

[6] L3 Collaboration, M.Acciarri et al.: CERN-PPE/94-45 March 1994.

[7] D.Bardin et al.: Phys.Lett. B308(1993)403.

[8] JADE Collaboration, W.Bartel et al.: Z.Phys. C33(1986)23.

[9] Y.Dokshizer: J.Phys. G17(1991)1441.

[10] S.Bethke et al.: Nucl.Phys. B370(1992)310.

[11] T.Sjostrand: Comp.Phys.Comm. 28(1983)227.

[12] S.L.Wu: Z.Phys. C9(1981)329.

[13] T.Muta et al.: Mod.Phys.Lett. A1(1986)203.

[14] O.Nicrosini and L.Trentadue: Phys.Lett. B196(1987)551.

[15] S.Banerjee, S.N.Ganguli, A.Gurtu and K.Sudhakar: TIFR/EHEP 94-4, April 1994.

[16] T.Aziz et al.: L3 Note #1474, August 28, 1993.

[17] S.N.Ganguli and K.Sudhakar: L3 Note #1496, September 17, 1993.